doi.org/10.15392/2319-0612.2025.2859
Braz. J. Radiat. Scci., Rio de Janeiro
2025, 13(2A) | 01-15 | e2859
Submitted: 2025-02-06
Accepted: 2025-05-14

Impact of computed tomography parameters on radiation dose in chest imaging: a comparative study between tomographs

Felix[ab], W. F.; Batista [b]. A.S.M.; Oliveira [b]. A.H; Abrantes [c] M.E.S.

[a] Hospital da Clínicas-UFMG/ Rede Ebserh, 30130-100, Belo Horizonte, Minas Gerais, Brasil.
[b] Universidade Federal de Minas Gerais, CEP: 31.270-901 Belo Horizonte, Minas Gerais, Brasil
[c] Pontifícia Universidade Católica de Minas Gerais, CEP: 30535-901, Belo Horizonte, Minas Gerais, Brasil - Correspondence: warleyferreirafelix@gmail.com

Abstract: due to the declaration of the Covid-19 pandemic by the World Health Organization in 2020, there was a significant increase in imaging exams to evaluate lung problems, these being the organs most affected by the disease. Given this demand, it is essential to understand how changes in the basic parameters of tomography exam protocols influence the doses of ionizing radiation received by patients. For this study, two test objects were used, one filled with water and the other with water containing areas of different densities. The study was carried out with a scan length of 70 mm each, to check variations in Hounsfield Units (HU) between exam protocols through statistical analyzes using the SPSS 21 software. For this purpose, scans were carried out on chest protocols routine on two computed tomography scanners from the same manufacturer, one with 4 rows and the other with 64, but with different tomographic image acquisition parameters. The scanning parameters used in the 64 rows tomograph were voltage of 120 kVp, modulated electric current, X-ray tube rotation time of 0.5 second, slice thickness of 2.0 mm, intervals between slices of 1.0 mm and spiral pitch of 0.828 and in the tomograph 4 rows, voltage 120 kVp, modulated electric current, X-ray tube rotation time of 0.75 seconds, slice thickness of 4.0 mm, interval between slices of 2.0 mm, spiral pitch of 1.0. The comparative results of the doses in the CT scanners showed that, in the 4 rows CT scanner, the total milliampere seconds (mAs) was 15.43% and the scanning time was 52.33% longer compared to the 64 rows CT scanner. However, the volume-weighted computed tomography dose index value ($CTDI_{VOL}$), the dose-length product (DLP) and the effective dose (E) were, respectively, 34.74%, 49.46% and 50.46% lower in the 4 rows tomography scanner compared to the 64 rows tomography scanner, which leads us to identify which parameters of the tomographic examination contribute to this 50% reduction in the effective dose between the tomography scanners. The identification of these parameters in protocols will reference the development of protocols with low doses of ionizing radiation, which will allow the optimization of exposure of patients who require evolutionary monitoring of pathologies through tomographic images.

Keywords: Covid-19, Low Dose of Ionizing Radiation, Chest Computed Tomography, Diagnostic Reference Levels.

doi.org/10.15392/2319-0612.2025.2859
Braz. J. Radiat. Scci., Rio de Janeiro
2025, 13(2A) | 01-15 | e2859
Submitted: 2025-02-06
Accepted: 2025-05-14

Impacto dos parâmetros da tomografia computadorizada na dose de radiação em exames de imagem de tórax: um estudo comparativo entre tomógrafos

Resumo: Em função da declaração da pandemia de Covid-19 pela Organização Mundial da Saúde em 2020, houve um aumento significativo na realização de exames por imagem para avaliação de problemas pulmonares, sendo esses os órgãos mais afetados pela doença. Dada essa demanda, é fundamental entender como alterações nos parâmetros básicos dos protocolos de exames de tomografia influenciam as doses de radiação ionizante recebidas pelos pacientes. Para este estudo foram utilizados dois objetos testes, um preenchido com água e outro com água contendo áreas de densidades diferentes. O estudo foi realizado com 70 mm de comprimento de varredura em cada, para checagem das variações de Unidades de Hounsfield (HU) entre os protocolos de exames por meio de análises estatísticas utilizando o software SPSS 21. Para isso foram realizadas varreduras em protocolos de tórax rotina em dois tomógrafos computadorizados do mesmo fabricante sendo um com 4 canais e o outro com 64, mas com parâmetros tomográficos de aquisição de imagens diferentes. Os parâmetros de varredura utilizados no tomógrafo de 64 canais foram, tensão de 120 kVp, corrente elétrica modulada, tempo de rotação do tubo de raios X de 0,5 segundo espessura de corte de 2,0 mm, intervalos entre cortes de 1,0 mm e Spiral pitch de 0,828 e no tomógrafo 4 canais, tensão 120 de kVp, corrente elétrica modulada, tempo de rotação do tubo de raios X de 0,75 segundo, espessura do corte de 4,0 mm, intervalo entre cortes de 2,0 mm, Spiral pitch de 1,0. Os resultados comparativos das doses nos tomógrafos apontaram que, no tomógrafo de 4 canais, o total de miliampere segundo (mAs) foi 15,43% e o tempo de varredura 52,33% maiores em comparação com o tomógrafo de 64 canais. Entretanto, o valor índice de dose em tomografia computadorizada ponderada por volume ($CTDI_{VOL}$), o produto dose comprimento (DLP) e a dose efetiva (E) foram, respectivamente, 34,74%, 49,46% e 50,46% menores no tomógrafo de 4 canais em comparação ao tomógrafo 64 canais, o que nos leva a identificar quais parâmetros do exame tomográfico contribuem para essa redução de 50% da dose efetiva entre os tomógrafos. A identificação destes parâmetros em protocolos, referenciará a elaboração de protocolos com baixa dose de radiação ionizante, que permitirá a otimização da exposição dos pacientes que necessitam de acompanhamento evolutivo de patologias através de imagens tomográficas.

Palavras-chave: Covid-19, Baixa Dose de Radiação Ionizante, Tomografia Computadorizada de tórax, Níveis de Referência Diagnóstica.

1. INTRODUCTION

Computed tomography (CT) is a necessary tool to assist in medical diagnosis as it provides detailed images that help in the discovery, treatment and monitoring of various clinical conditions of patients. However, the high dose of ionizing radiation emitted by CT has raised concerns among entities promoting radioprotection. Studies indicate that CT, although representing only 10% of all medical exposures, is responsible for more than 60% of the collective effective dose. Comparatively, a chest CT exposes the patient to an average dose of 10 mSv, while a PA chest X-ray exposes the patient to only 0.1 mSv on average [1, 2].

Studies have shown that exposures increase the probability of inducing cancer even at low doses, with a 4% increase in the risk of cancer-related death for each 1.0 sievert (Sv) increase in the effective dose. The Covid-19 pandemic caused a sharp increase in the use of chest CT for diagnosis and monitoring of pathology, further increasing exposure to ionizing radiation. Given this situation, it is essential to optimize radioprotection planning, aligning it with the objectives of medical exposure to minimize absorbed radiation doses without compromising diagnostic quality [3, 4].

Routine chest CT protocols have an effective dose of 8.0 to 10.0 mSv, while studies suggest that low dose protocols should be less than 2.5 mSv. Low dose protocols for CT are not yet well defined quantitatively in the literature, making it difficult to standardize them, which is so necessary in the post-covid-19 pandemic context [5, 6].

The lack of standardization of Diagnostic Reference Levels (DRL) for CT exams causes uncertainty in the definition of dose standards for chest CT in routine protocols, making it difficult for agencies promoting radioprotection to establish parameters for low dose exams [7, 8, 9]. In this sense, this study aims to compare the effective dose between routine chest CT protocols from two tomographs and discuss the need to establish DRLs, which will serve as references for the development of low dose CT protocols, aiming to reduce the dose of ionizing radiation and promote more optimized medical exposures.

2. METHODOLOGY

In ANVISA normative instruction 93 (IN 93), in its annex II, the maximum references for representative dose values in medical CT are established, presenting the references only for three types of exams, head and abdomen (typical adult)[1] and abdomen (pediatric)[2] [10]. On the Table. 1 presents $CTDI_{VOL}$, DLP and effective dose values for chest CT, established by radiological protection regulatory agencies in several countries.

Table 1: Reference values for $CTDI_{VOL}$, DLP and effective dose.

Countries or Regulatory Agency	$CTDI_{VOL}$ (mGy)	DLP (mGy.cm)	Effective dose (mSv)
United Kingdom [7]	-	-	14
USA [7]	-	-	6.1
Russia [7]	-	-	6.3
United Kingdom [8]	14	580	8.1
Europe [8]	30	650	9.1
IAEA [8]	9.5	447	6.3
Korea [8]	15	550	7.7
ACR [9]	12	443	6.2
NCRP [9]	21	-	-
Japan [9]	15	550	7.7
European Union [9]	10	400	5.6
United Kingdom [9]	12	610	8.5
Ireland [9]	9	390	5.5
Australia [9]	15	450	6.3
Canada [9]	14	521	7.3
Saudi Arabia [9]	5	190	2.7
Greece [9]	14	480	6.7

[1] Weight between 60 and 75 kg and height of 1.60 to 1.75 m.
[2] Individual aged 5 years, weighing approximately 20 kg.

After the publication of this IN 93, it became mandatory to provide $CTDI_W$ or $CTDI_{VOL}$ and DLP in standard DICOM images of all tomographic exams [10].

The main ionizing radiation dose indices for tomographic examinations are provided in the dose reports for each tomographic examination and presented below:

• $CTDI_{VOL}$ (The Volume Computed Tomography Dose Index): measured in mGy, represents a dose estimate adjusted to the scanned volume.

• DLP (Dose-Length Product): measured in mGy.cm, it is the product of $CTDI_{VOL}$ and the length of the exam.

• Effective Dose (E): is the product of the DLP and a specific constant (k) for each region of the human body scanned (for chest, k = 0.014 mSv/mGy.cm), measured in mSv [2, 7].

These indices are used as a reference for optimization and radioprotection in tomographic examinations. In this study, the effective dose was adopted to compare doses between different exam protocols [11, 12, 13, 14]

The study evaluated chest scanning protocols (routine)[3] on two CT scanners, and the basic parameters are presented on table 2, and were taken from the details of protocols.

Table 2: Basic parameters chest scanning protocols

Parameters	**Tomographs**	
	64 rows	**04 rows**
kVp	120	120
Electric current (mA)	modulated	modulated
X-ray tube rotation time (s)	0.50	0.75
Slice thickness (mm)	2.0	4.0
Interval between slices (mm)	1.0	2.0
Spiral pitch	0.828	1.000

[3] Protocol for the study of rib cage tissues that covers most of the clinical indications for carrying out a tomographic examination of the structure.

These are the main parameters of thoracic pathology assessment protocols.

To understand how changes in the basic parameters of routine protocols for chest CT reflect the variation in effective dose, a pilot study was carried out on two CT scanners from the manufacturer Canon Medical (Toshiba).

Test objects supplied with the CT scanners and used in quality control and calibration tests were used, by checking variations in the Hounsfield Units (HU) with standards provided by the manufacturers.

For the pilot test, the routine protocol for chest scanning was used on both tomographs, with a scan length of 70 mm on both test objects.

The test objects used were the Water Phantom filled with water, Fig. 1, in a cylindrical format of 330 mm in diameter and 90 mm in height and the TOS Phantom, Fig. 2, with areas of varying densities and filled with water, in a cylindrical 330 mm in diameter and 100 mm in height.

The readings on the images of the test objects were carried out using the Horos software [15] and the HU value reading tool (ROI)[4] was used, in an elliptical shape and with an equal area for each measurement.

In the water phantom, the ROIs were distributed like the hours of a clock to verify the uniformity of the HU values in the test object.

4 Region Of Interest.

Figure 1: Position ROI`s in Water Phantom

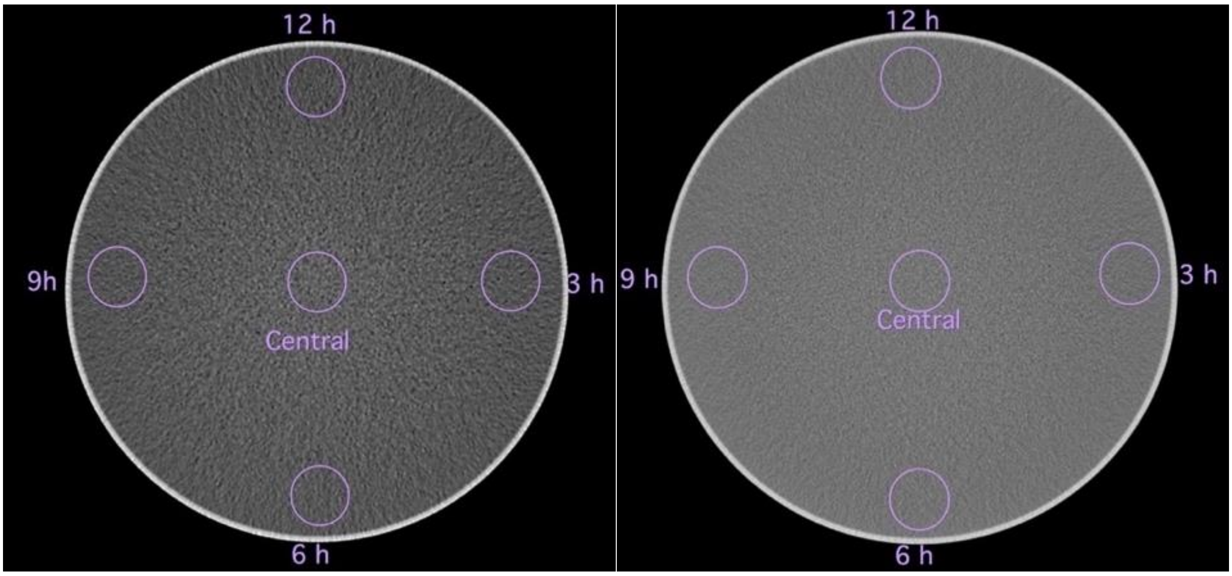

Source: owner; left TC 64 row, right TC 04 rows.

In TOS Phantom, Fig. 2, the ROIs present the same size and shape. The ROIs were positioned in each region so that they fit completely within the studied area so as not to go beyond the limits of the regions, causing interference in the measurements.

Figure 2: Position ROI`s in TOS Phantom.

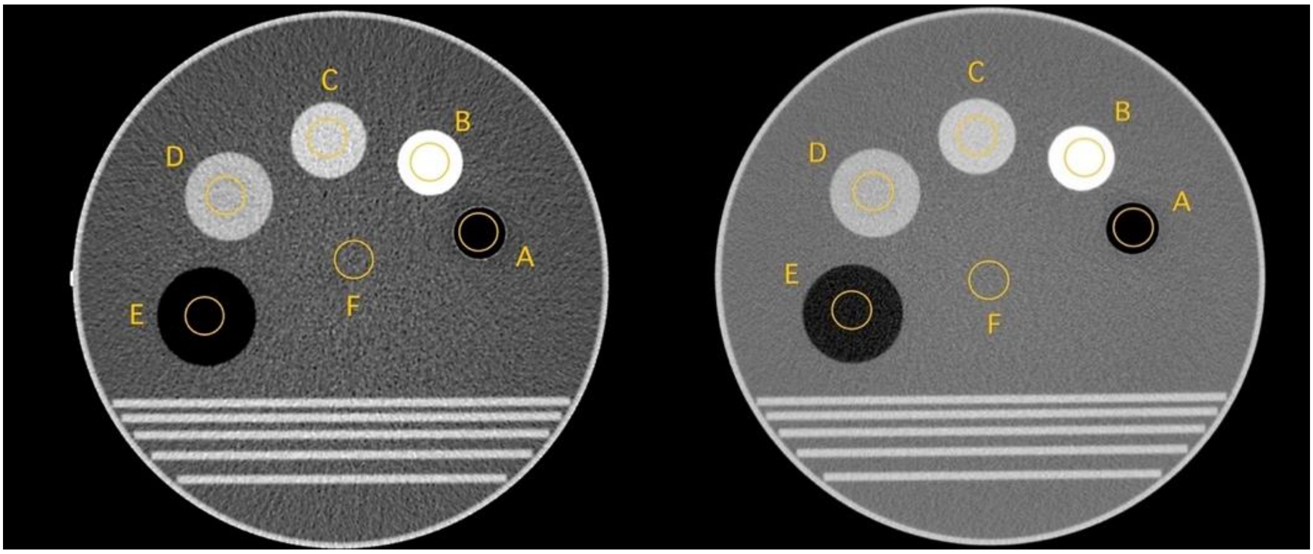

Source: owner; left TC 64 row, right TC 04 rows.

The values of the readings obtained in the test objects were subjected to statistical tests to evaluate these data, presenting the average and standard deviations, evaluation of the dispersion of the data in relation to the average through the coefficient of variation, the analysis of statistical significance of the differences of the average using the paired two-sample t-test and finally measuring the degree of linear correlation between two variables using the Pearson correlation coefficient [16].

The analyses were performed using IBM SPSS 21 software [17] and the results are presented in section 3.

3. RESULTS

Statistical analysis of the data obtained are presented in tabs. 2, 3, 4 and 5, where (N) is the number of slices from which measurements were taken on the phantom, the average and standard deviation (SD) of the samples, coefficient of variation (CV) expressed as a percentage, p-value and Pearson's Correlation coefficient (r).

Below in table 3, the descriptive statistics of the HU values read in the water phantom in the tomography are presented.

Table 3: Water Phantom statistical data

64 ROWS	12H	3H	6H	9H	CENTRAL
N	27	27	27	27	27
Average	-13.83	-11.35	-6.81	-10.62	-0.59
SD	0.87	0.48	0.57	0.21	0.50
CV (%)	-0.06	-0.04	-0.08	-0.02	-0.84
04 ROWS	**12H**	**3H**	**6H**	**9H**	**CENTRAL**
N	26	26	26	26	26
Average	-11.34	-8.98	-3.84	-6.24	0.35
SD	0.40	0.22	0.58	0.33	0.50
CV (%)	-0.03	-0.02	-0.15	-0.05	1.42

The coefficient of variation presented small values indicating a low dispersion of the data in relation to the average.

Table 4 presents the results for p-value and Pearson's correlation coefficient of the data obtained in the water phantom in both tomography devices.

Table 4: Correlations between CT regions 64 rows x 04 rows in the water phantom

64 ROWS *X* 04 ROWS	12H	3H	6H	9H	CENTRAL
N	26	26	26	26	26
p-value	0.09	0.12	0.04	0.45	0.17
Pearson´s Correlation coefficient (r)	0.34	0.31	0.41	0.16	0.28

In the analysis of the p-value, the 12 h, 3 h, 9 h and central positions present values greater than 0.05, indicating the absence of significant statistical differences when comparing the data obtained from the tomographs. At the 6 h position, the statistical difference is significant in this group

Pearson's Correlation coefficient between the 12 h, 3 h and 6 h positions has a weak linear correlation, while the 9 h and central positions have nonlinear correlation.

Table 5 below presents the descriptive statistics of the TOS phantom.

Table 5: TOS Phantom statistical data

64 ROWS	A	B	C	D	E	F
N	38	38	38	38	38	38
Average	-968.84	328.42	117.47	82.51	-106.68	-0.94
SD	0.66	1.48	0.84	0.61	0.45	0.72
CV (%)	-0.0007	0.0044	0.007	0.0074	-0.004	-0.77
04 ROWS	**A**	**B**	**C**	**D**	**E**	**F**
N	28	28	28	28	28	28
Average	-984.68	354.38	119.98	85.30	-105.98	0.13
SD	0.59	1.09	0.62	1.13	0.30	0.25
CV (%)	-0.0006	0.0030	0.0051	0.0132	-0.0027	1.97

In the TOS phantom, it is also observed that the coefficient of variation presented small values in the studied regions, indicating a low dispersion of the data in relation to the average.

Table 6: Correlations between CT regions 64 rows x 04 rows in the TOS phantom

64 ROWS X 04 ROWS	A	B	C	D	E	F
N	28	28	28	28	28	28
p-value	0.95	0.38	0.26	0.68	0.38	0.84
Pearson´s correlation coefficient (r)	-0.01	0.17	0.22	0.08	0.17	-0.04

Evaluating the statistical differences between the groups by analyzing the p-value, they indicate that in positions A, B, C, D, E and F, values greater than 0.05 demonstrate the absence of significant statistical differences when comparing the data obtained.

The Pearson's correlation coefficient between positions A, B, C, D, E and F shows a nonlinear correlation.

Data from the pilot study as described in the methodology, carried out with the Water Phantom, were extracted from the CT scanner dose report and the effective dose was calculated. These data were tabulated and presented in Table 7.

Table 7: - Data obtained in the preliminary test.

Dose parameters	Tomograph (Chest routine)		
	64 rows	**04 rows**	**Difference %**
Scan Length (mm)	70	70	-
Total mAs	1595	1841	15.43
Scan Time (s)	6.86	10.45	52.33
$CTDI_{VOL}$ (mGy)	38.00	24.80	-34.74
DLP (mGy.cm)	537.80	271.80	-49.46
Effective Dose (mSv)	7.53	3.80	-50.46

It is observed that the 4 row CT scanner presents a total of mAs 15.43% higher, that may be justified by the fact that the scan time is longer, a scanning time 52.33% longer, because the X-ray tube rotation time is 50% longer than the 64 row CT scanner, a $CTDI_{VOL}$, 34.74% lower and the DLP is 49.46% lower and the effective dose value is 50.46% lower, compared to the 64 row CT scanner. The ionizing radiation dose indices for tomographic exams are lower and are directly related to an increased X-ray tube rotation time, causing a reduction in mA, and with a spiral pitch of 1.000, eliminates the overlap between slices; these are possible factors for a lower ionizing radiation dose in the 4 row CT scanner. The statistical tests performed on the test objects indicate a low dispersion of the data in relation to the averages, with no significant statistical differences and weak or null linear correlations. Such result shows that the variations in the data were not significant and that the quality of the images in the CT's are equivalent, therefore both tomographies present diagnostic quality for carrying out examinations.

Therefore, since the reference dose measurements for the 4-slice CT scanner were lower than those for the 64-slice scanner, it is proposed that the basic parameters of the routine chest protocol used in the 4-slice scanner could serve as a basis for developing a low-dose protocol, while assessing the adequate preservation of image quality.

In the context of radiological protection, using references that reduces the dose in tomographic examinations by 50% with image quality for diagnosis, has a positive impact on planning the optimization of the dose of ionizing radiation in patients, especially in sequenced examinations that are often necessary for monitoring pathologies.

4. CONCLUSIONS

The statistical tests indicated that for the Water Phantom in both tomographs the coefficients of variation present low data dispersion in relation to the average, showing no statistically significant differences in the 12 h, 3 h, 9 h and Central positions and having a significant statistical difference in the position 6 h, showing a weak linear representation coefficient at positions 12 h, 3 h, 6 h and nonlinear correlation coefficient at 9 h and Central.

The statistical tests presented for the TOS Phantom in both tomographs show low dispersion of the data in relation to the average, with no statistical differences revealed in the regions and the linear correlation coefficient in the regions is null.

As shown, small differences between the basic parameters of chest tomographic scanning protocols, in the tomographs presented in this study, can result in a reduction of up to 50% in the effective dose.

A clear definition of Diagnostic Reference Levels of ionizing radiation for tomographic examinations is essential for effective planning aimed at reducing dose and optimizing radioprotection for patients.

Additionally, it is important to objectively establish well-defined concepts of Diagnostic Reference Levels to guide the creation of protocols that use low doses of ionizing radiation.

The development of low dose ionizing radiation protocols in tomographic examinations is of great importance in the process of optimizing and planning radioprotection, providing lower exposure and contributing to the reduction of individual effective doses and, consequently, collective effective doses.

ACKNOWLEDGMENT

To the Hospital das Clínicas of the Universidade Federal de Minas Gerais - rede Ebserh, in particular to manage the Diagnostic Imaging Unit for enabling this research to be carried out.

To the Department of Nuclear Engineering at the School of Engineering of the Universidade Federal de Minas Gerais, for the educational support.

The authors are grateful to the Comissão Nacional de Energia Nuclear (CNEN), the Coordenação de Aperfeiçoamento de Pessoal de Nível Superior (CAPES), the Fundação de Amparo à Pesquisa do Estado de Minas Gerais (FAPEMIG) and the Conselho Nacional de Desenvolvimento Científico e Tecnológico (CNPq) for the support.

CONFLICT OF INTEREST

Warley F. Felix is an employee in Hospital da Clínicas-UFMG/ Rede Ebserh.

The remaining authors have no conflicts of interest to declare.

REFERENCES

[1] J. Ford, Radiation, people and the environment. (2004). https://inis.iaea.org/search/search.aspx?orig_q=RN:35041876 acessado em 01/2022.

[2] UNSCEAR, Sources, Effects and Risks of Ionizing Radiation, United Nations Scientific Committee on the Effects of Atomic Radiation (UNSCEAR) 2020/2021 Report: Report to the General Assembly, With Scientific Annexes A and B. UN (2022).

[3] P. P. Silva e A. L. Marcondes, Otimização da dose de radiação ionizante em tomografia computadorizada. Tekhne e Logos, Vol. 9, n. 1, pp. 88-98 (2018).

[4] S. Andresz, *et al.* Optimization of radiation protection: Alara, a practical guidebook (2019).

[5] J. Azadbakht, *et al.* A review on chest CT scanning parameters implemented in COVID-19 patients: bringing low-dose CT protocols into play. Egyptian Journal of Radiology and Nuclear Medicine, Vol. 52, pp. 1-10 (2021).

[6] M. Tækker, *et al.* Diagnostic accuracy of low-dose and ultra-low-dose CT in detection of chest pathology: a systematic review. Clinical Imaging, Vol. 74, pp. 139-148 (2021).

[7] J. D. Harrison, *et al.* The use of dose quantities in radiological protection: ICRP publication 147 *Annals of the ICRP* 50 (1) 2021. Journal of Radiological Protection, Vol. 41, n. 2, p. 410 (2021).

[8] L. T. Dauer, *et al.* (Ed.). Dose, benefit, and risk in medical imaging. CRC Press (2018).

[9] S. K. Albahiti *et al.* Establishment of institutional diagnostic reference levels for 6 adult computed tomography examinations: Results from preliminary data collection. Radiation Physics and Chemistry, Vol. 201, p. 110477 (2022)

[10] BRASIL. Instrução Normativa Nº 93 de 27 de maio de 2021. Estabelece os requisitos sanitários para a garantia da qualidade e da segurança em sistemas de tomografia computadorizada médica. (2021). https://www.in.gov.br/en/web/dou/-/instrucao-normativa-in-n-93-de-27-de-maio-de-2021-323016253 acessado em 01/2022.

[11] J. D. Harrison. *et al.* ICRP publication 147: use of dose quantities in radiological protection. *Annals of the ICRP*, Vol. 50, n. 1, pp. 9-82 (2021).

[12] T. C. Alonso. Dosimetria em tomografia computadorizada e avaliação das doses nos órgãos em varreduras de tronco (2016)

[13] J. Hsieh, *et al.* Computed tomography: principles, design, artifacts, and recent advances. In: Bellingham, Washington USA (Published by SPIE and John Wiley & Sons, Inc.): SPIE, (2022).

[14] A. P. Mourão. Tomografia computadorizada: tecnologias e aplicações. São Caetano do Sul, SP: Difusão, (2017).

[15] HOROS. Versão 3.3.6. Disponível em: https://horosproject.org/download

[16] VIEIRA, Sônia. Introdução à bioestatística. GEN Guanabara Koogan, 2021

[17] IBM Corp. Released 2012. IBM SPSS Statistics for Macintosh, Version 21.0. Armonk, NY: IBM Corp.

LICENSE